Steel and Composite Structures, *Vol. 54, No. 1 (2025) 1-15*
https://doi.org/10.12989/scs.2025.54.1.001

Development of an innovative cold-formed steel-plywood composite floor system using epoxy-resin adhesive for residential buildings

Miqdad Khosyi Akbar[b], Ali Awaludin[*] and Andreas Triwiyono[a]

Department of Civil & Environmental Engineering, Faculty of Engineering, Gadjah Mada University, Indonesia

(Received June 30, 2024, Revised December 27, 2024, Accepted December 30, 2024)

Abstract. This study aimed to develop innovative lightweight composite flooring system consisting of cold-formed steel (CFS) and plywood with epoxy-resin adhesive connections. During the investigation, four composite floor panels were fabricated by bonding C75.100 CFS beams with 12 mm thick Meranti plywood on bottom flange and 18 mm thick Meranti-Sengon plywood on top flange using epoxy-resin adhesive. These panels have dimensions of 900 mm by 2800 mm, with a thickness of 105 mm, and were subjected to vibration, bending, and creep tests. In addition, evaluation of the floor system was conducted to determine its compliance with the required ultimate and serviceability limit states, based on typical residential building design loads. Numerical analysis were developed to validate the vibration and bending test results. The experimental results for the floor system showed natural frequency of 25.65 Hz, moment capacity of 18.60 kNm, flexural stiffness of 369.96 kNm², and 90th-day creep factor of 0.15. Numerical analysis differences compared to experimental results were in acceptable ranges, including 0.4–10.6% for moment capacity, 3.3–5.5% for flexural stiffness, and 6.2–7.4% for natural frequency. Following this discussion, safety factor of 6.2 was obtained from ultimate limit state evaluation. Total deflection, including 0.24 creep factor for 50-year service life, was 4.88 mm, less than 1/240 of floor span limit. The natural frequency of 25.65 Hz exceeded the minimum comfort requirement of 8-9 Hz. The results of the investigation showed that this CFS-plywood composite floor system was lightweight, safe, and suitable for residential buildings.

Keywords: complex networks; mathematical simulation; mechanical behavior; nanotechnology

1. Introduction

Cold-formed steel (CFS) is typically used primarily as roof trusses in residential buildings. However, after the 2018 Lombok earthquake in Indonesia, its high strength-to-weight ratio led to its use as the primary structural material in residential buildings, notably in the Rumah Instan Sehat Baja Ringan (RISBARI) (Awaludin *et al*. 2020). Cold-formed steel construction offers the advantage of producing 30% lower carbon emissions than hot-rolled steel construction (Johnston *et al*. 2018) and 33% lower than concrete construction (Altmann *et al*. 2022). Furthermore, to achieve better structural performance, CFS may also be combined with concrete as a composite column (Lai *et al*. 2024, Lai *et al*. 2024), beam (Valsa Ipe *et al*. 2013), and floor system (Omar A. Shamayleh and Harry Far 2022).

The structural behavior of composites, particularly under bending loads, has been widely studied to optimize design and performance. Różyło (2023) conducted experimental and numerical investigations on composite beams subjected to three-point bending. The study provided insights into failure mechanisms, emphasizing the role of damage initiation and progression in composite materials. Similarly, Szewczak *et al*. (2020) explored CFS sigma beams retrofitted with CFRP tapes under four-point bending, demonstrating that such reinforcement improved both bending capacity and stiffness. These studies highlight the significance of evaluating bending behavior in composite systems to enhance their structural efficiency. Research on CFS composite floor systems under bending loads has also explored the integration of wood panels for environmental and structural benefits (Dheeraj Karki *et al*. 2022). Wood panels, as alternatives to concrete, reduce carbon and greenhouse gas emissions, which are significantly generated by the cement industry (Meyer 2013, Pratiwi and Tjondro 2018). This combination produces lightweight, sustainable flooring systems that are easy to fabricate manually without heavy equipment.

Some research on composite floor systems using CFS and wood-based panels have been extensively developed. CFS joists, with a spacing of 600 mm, were compositely connected to the particle board using self-drilling screws (Kyvelou *et al*. 2015, Raffoul *et al*. 2019). The results showed that using particle board increased the moment capacity and flexural stiffness by 100% and 40%, respectively, compared to bare CFS systems. Al Hunaity *et al*. (2022) examined the vibration of a CFS-particleboard composite floor system through numerical analysis. The results showed that the natural frequencies of this floor system were higher than the minimum limits given in three standards, namely Australian Standard AS 3623 (Australian

*Corresponding author, Ph.D.
E-mail: ali.awaludin@ugm.ac.id
[a]Professor
E-mail: andreas.triwiyono@ugm.ac.id
[b]M.Eng. Student
E-mail: miqdadkhosyiakbar@mail.ugm.ac.id

ISSN: 1229-9367 (Print), 1598-6233 (Online)

Standards 1993), AISC design guide 11 (American Institute of Steel Construction 2011), and Eurocode 5 (EN 1995-1-1 2004). However, considering that the particle board is classified as a low-density fiberboard (LDF), the increase in moment capacity and flexural stiffness can still be improved. Karki *et al*. (2021) conducted a numerical study on composite floor systems using CFS with various types of wood panels, including particle board, oriented strand board (OSB), plywood, laminated bamboo, and laminated veneer lumber (LVL). The numerical analysis showed that moment capacity and flexural stiffness increased with the modulus of elasticity of the wood panel used. LVL and plywood panels achieved the highest moment capacity in CFS composite floor systems, surpassing particle board by 4.5%. Therefore, using plywood as timber boards in CFS composite flooring systems could be a new experimental research development.

Besides the material of the composite flooring system, understanding connection behavior, in terms of their strength and stiffness, is critical to accurately predicting the performance of composite structures (Hassanieh *et al*. 2017, Wusqo *et al*. 2019). Mechanical fasteners, such as self-drilling screws, are commonly found in structures utilizing CFS. However, using self-drilling screws alone provides relatively low stiffness, so adding epoxy-based adhesive to the surface of the CFS and the connected panel can increase the stiffness of the connection (Karki *et al*. 2022). A previous study has compared the behavior of two types of CFS-plywood composite connections—self-drilling screws and epoxy-resin adhesive alone—through single-shear tests in the laboratory (Akbar *et al*. 2024). The test results demonstrated that a plywood board connected to a CFS beam using epoxy-resin adhesive connections could produce a significantly higher stiffness than self-drilling screw connections. Moreover, the use of adhesive connections provides a more aesthetic appearance by reducing the imperfection on the surface of the flooring systems compared to self-drilling screw connections.

In a floor system design, the ultimate and serviceability limit states are two aspects that need to be examined. Some research conducted in recent years have been primarily focused on assessing moment capacity and deflection due to short-term loading, either through laboratory tests or numerical analysis (Far 2020, Kyvelou *et al*. 2018, 2021). However, according to Ngudiyono *et al*. (2020), in materials with high viscosity, such as wood, their structural capacity also depends on the loading duration. Although the applied load may be relatively constant, increased deformation can occur if the load is applied for a long-term duration. This phenomenon is known as creep (Kullit 2013). Therefore, the creep behavior needs to be considered in the serviceability design of structures utilizing wood-based materials (Nashirudin *et al*. 2016). Currently, there is very limited research on the creep behavior of CFS-wood panel floor systems, highlighting the need for laboratory testing.

Vibration was another aspect that needed to be checked in evaluating serviceability limit states of flooring systems. Combining CFS with plywood as a lightweight flooring system could cause vibration issues that impact users' comfort activities (Al Hunaity *et al*. 2022). Several common human activities can exert dynamic forces on the floor system within specific frequency ranges. Rhythmic activities, such as dancing, aerobic exercises, or cheering at events with many spectators, could lead to resonance amplification (Allen and Rainer 1976). Therefore, Eurocode 5 (EN 1995-1-1 2004) and AISC design guide 11 (AISC 2016) provided minimum limits for the natural frequency of a floor system to prevent this issue.

Unlike previous studies that focused primarily on short-term mechanical performance or specific test, this study provides a comprehensive investigation into the behavior of CFS-plywood composite flooring systems. The use of epoxy-resin adhesive connections as an alternative to traditional fasteners addresses both aesthetic and structural limitations identified in prior research. Moreover, the study's holistic approach, combining vibration, bending, and creep testing with numerical validation, contrasts with existing work that often examines these aspects in isolation. This integrated methodology contributes new insights into the long-term serviceability and ultimate performance of such flooring systems, advancing both theoretical understanding and practical applications.

This study aims to develop an innovative composite flooring system consisting of CFS and plywood with epoxy-resin adhesive connections. The developed composite flooring system behavior was then investigated through comprehensive laboratory tests, including vibration, bending, and creep tests, to determine its natural frequency, moment capacity, flexural stiffness, and creep factor. In addition, numerical models were developed to validate the natural frequency, moment capacity, and flexural stiffness obtained from vibration and bending tests. Subsequently, ultimate and serviceability limit state evaluations were performed to assess the ability of the floor system to support the design loads in residential buildings.

Table 1 Material properties of cold-formed steel

Material	Yield strength, f_y (MPa)	Modulus of elasticity, E_s (MPa)	Poisson's ratio
Cold-formed steel	619.54	200000	0.3

2. Material tests

Lipped C-section CFS, which commonly used in the construction industry (Ahmed Sheta *et al*. 2023), was used in this study. The material properties of CFS used were not tested in the laboratory but were obtained from previous investigations that applied the same material as in this study (Making *et al*. 2021). The material properties of CFS used were shown in Table 1. This study used two plywood materials, namely 12 mm thick Meranti plywood (*Shorea spp.*) and 18 mm thick combined Meranti (*Shorea spp.*) as well as (*Albizia chinensis*) plywood. For both plywood materials, coupons were extracted from the plywood panels and subjected to bending, compressive, as well as tensile tests parallel to the face grain of plywood according to EN

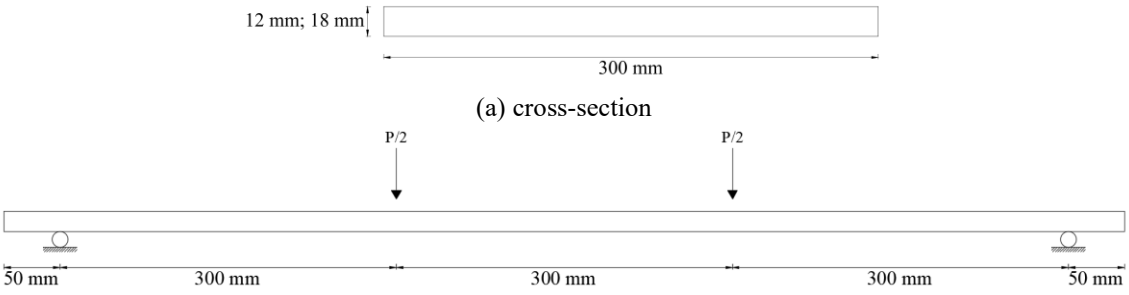

(a) cross-section

(b) elevation

Fig. 1 Dimensions of plywood bending test specimens

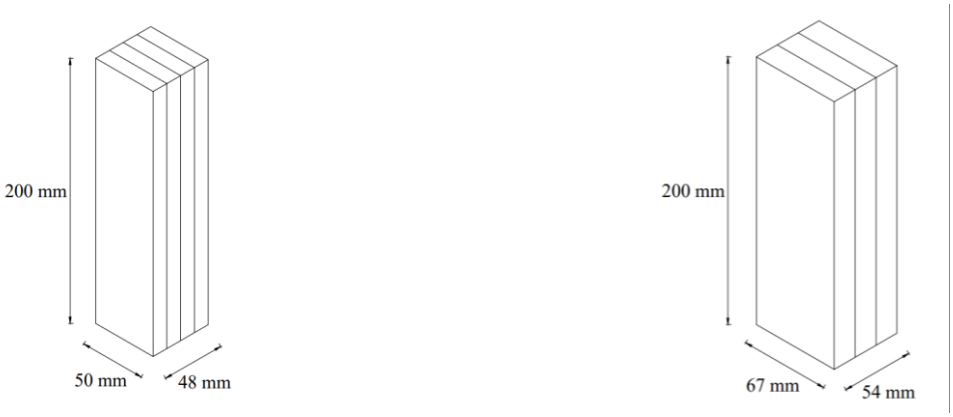

(a) 12 mm thick plywood (b) 18 mm thick plywood

Fig. 2 Dimensions of plywood compressive test specimens

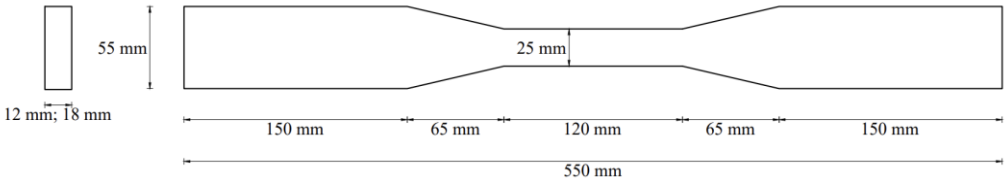

Fig. 3 Dimensions of plywood tensile test specimens

789 (EN 789 2004). Three repeated tests were conducted for each test type and both plywood types.

2.1 Plywood bending tests

Four-point bending tests were carried out to determine both plywood types' bending strength and modulus of elasticity. The dimensions of the specimens and the experimental set-up are presented in Fig. 1. A linear variable displacement transducer (LVDT) was placed on the top of the board to measure the vertical deflection during the test. The load was applied through a 300-kN universal testing machine (UTM) at a constant rate for approximately 300 seconds of test duration until failure occurred.

2.2 Plywood compressive and tensile tests

Compressive and tensile tests were conducted to determine the strength of each plywood type in these two loading directions. The dimensions of the compressive and tensile test specimens are illustrated in Figs. 2 and 3, respectively. For the compressive specimens, epoxy-resin adhesives were used to glue the coupons together. A 3000-kN compression testing machine and a 300-kN universal testing machine (UTM) were used to apply the load to the compressive and tensile test specimens. A constant loading rate was set so that the test lasted for approximately 300 seconds for each specimen. In addition, compressive test specimens were also used to measure the density of each plywood type.

2.3 Material test results

The key parameters, the density, modulus of elasticity, bending strength, compressive strength, and tensile strength obtained from the plywood material tests, were averaged from all specimens and presented in Table 2. It was found that the physical and mechanical properties of Meranti plywood were much higher than those of Meranti-Sengon plywood.

Table 2 Material properties of examined plywood

Plywood types	Thickness, t_b (mm)	Density, ρ (kg/m^3)	Modulus of elasticity, MoE (MPa)	Bending strength, f_{mb} (MPa)	Compressive strength, f_{cb} (MPa)	Tensile strength, f_{tb} (MPa)
Meranti	12	631.06	13364.95	32.36	25.01	28.69
Meranti-Sengon	18	395.65	6889.27	29.98	16.99	16.92

Table 3 Epoxy-resin adhesive shear strength and modulus

Bonded material	Plywood thickness, t_b (mm)	Adhesive shear strength, $f_{v,a}$ (MPa)	Adhesive shear modulus, G_a (MPa)
CFS-Meranti plywood	12	1.73	2.31
CFS-Meranti-Sengon plywood	18	2.17	2.51

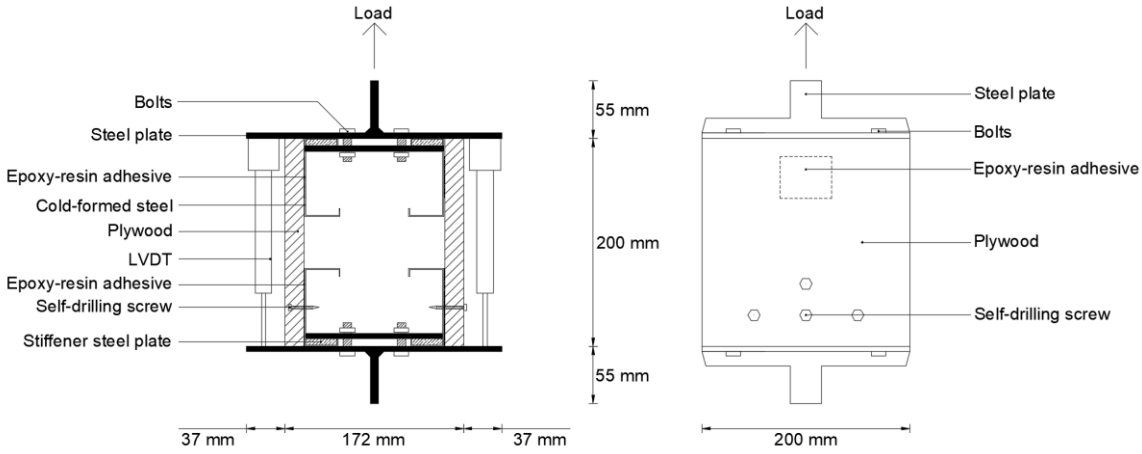

(a) cross-section (b) elevation

Fig. 4 Epoxy-resin adhesive single shear test set-up (Akbar *et al*. 2024)

3. Epoxy-resin adhesive shear tests

The strength and stiffness of epoxy-resin adhesive were obtained through single-shear tests. This test used tensile loading scheme to prevent buckling of the CFS. The test set-up referred to the study by Akbar *et al*. (2024), which was shown in Fig. 4. At the top side of the specimen, CFS was bonded to plywood using epoxy-resin adhesives with dimensions of 1 × 40 × 50 mm. Meanwhile, the bottom side of the specimen was connected using a combination of four self-drilling screws and epoxy-resin adhesive to prevent slip, allowing the slip measurement to be focused on the top side of the specimen. A 100-kN universal testing machine (UTM) was used to apply the load. At the same time, two LVDTs on both sides of the specimen were used to measure the slip that occurred.

The typical failure modes occurred on three specimens, namely brittle failures with partial detachment of wood fibers in the plywood outer layer and detachment of epoxy-resin adhesive from the CFS surface. The adhesive shear strength was calculated as the maximum load per shear area, and the shear modulus was derived from the load-slip relationship up to 40% of the maximum load. The results of normalized adhesive shear strength and modulus for each type of bonded plywood are presented in Table 3 and used as interaction properties of CFS-plywood interaction in the numerical model.

4. Composite floor tests

4.1 Test specimens

The specimen comprising four 3000-mm long C75.100 CFS supported with cross-section dimensions was shown in Fig. 5. Two plywood boards were used, including 12 mm thick Meranti plywood and 18 mm thick Meranti-Sengon plywood. Each plywood board had dimensions of 900 mm by 2400 mm. To produce a board of 3000 mm in length, including the same length as joists of CFS, the identical plywood boards were cut and jointed using epoxy-resin adhesive at two symmetrical locations, as shown in Fig. 5.

To prevent premature localized failure of CFS joists due to individual slenderness, cross-sections of CFS joists at the support and loading points were strengthened with 200-mm long timber blocks attached using self-drilling screws. Moreover, the two 3000-mm long plywood boards were bonded with four CFS joists on the bottom and top flange using 1-mm thick epoxy-resin adhesive. According to the product description, the curing process was conducted for a minimum of 3 days to achieve optimum adhesive strength. Following this discussion, the cross-section dimensions of the assembled specimen were shown in Fig. 5. A total of four identical specimens were fabricated for several tests. Three specimens were used for bending tests, considering the variability of timber materials, the specimen

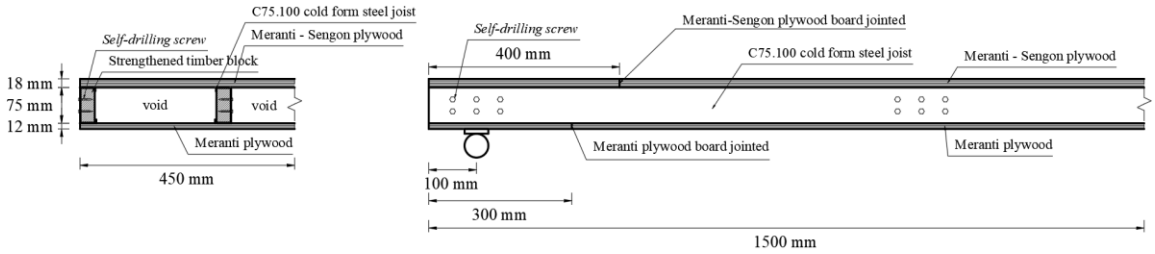

Fig. 5 Cross-section of C75.100 cold-formed steel joist

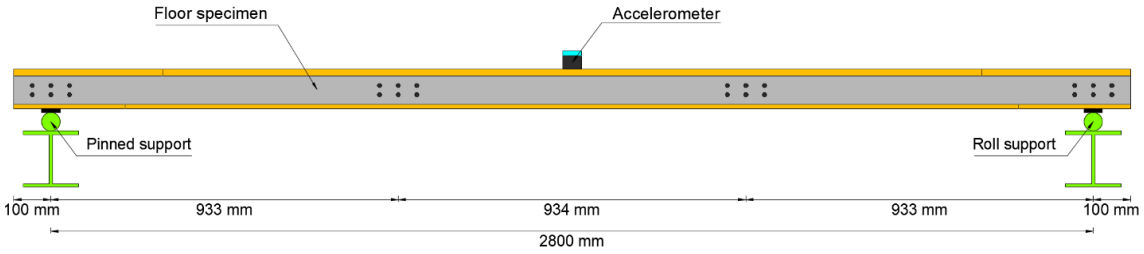

Fig. 6 Experimental layout for the vibration test

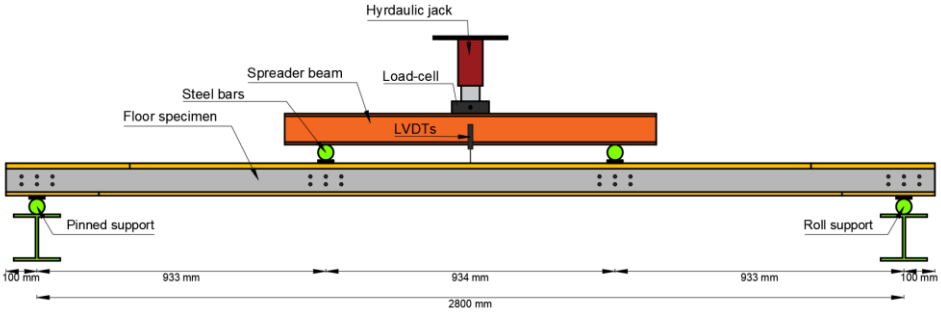

(a) Experimental layout

(b) Laboratory set-up

Fig. 7 CFS-plywood composite floor system four-point bending test

manufacturing process which was not guaranteed to be perfectly consistent, and the purpose of validation to the numerical modeling results. Meanwhile, one specimen was used for the vibration test followed by the creep test.

4.2 Vibration tests

About 2800-mm span of floor specimen and simply supported boundary condition were used in vibration tests to investigate the dynamic characteristics of flooring system. Welded-to-steel beam steel bar at the end of longitudinal floor specimen recognized the pin support, while free steel bar represented the roller support. This pinned-roll idealized support was also used in both bending and creep tests. During the process, a metal plate was bonded on floor specimen at the mid-span using epoxy

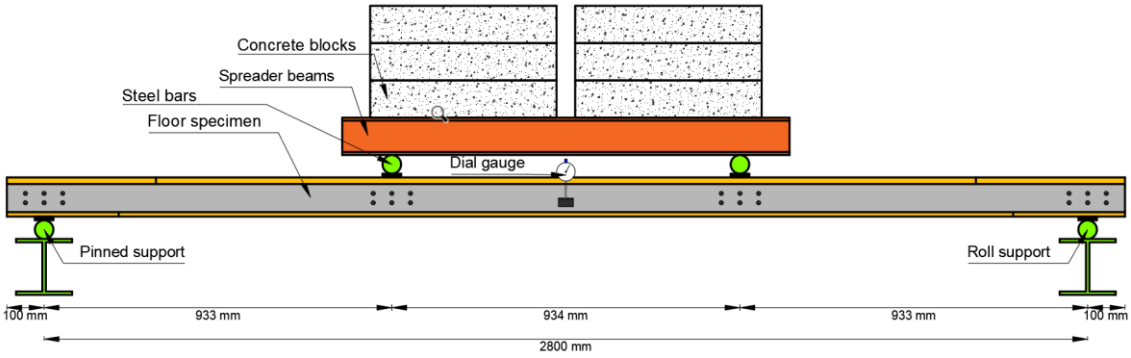

(a) Experimental layout

(b) Laboratory set-up

Fig. 8 CFS-plywood composite floor system creep test

adhesive, and accelerometer was attached to the plate with the magnetism of accelerometer. The experimental layout for vibration test in the investigation was shown in Fig. 6. Rubber hammer was used to excite the floor specimen, and the resulting free vibration response was recorded by the data logger during the study. Due to the limitation of the instrument, which was only able to record the response with a sampling rate of 100 Hz, the impact forces were applied at the mid-span of the specimen to excite the first flexural mode.

4.3 Bending tests

Three typical specimens were used for four-point bending test with simply supported boundary conditions as applied in vibration tests. Bending tests were conducted to assess the strength and stiffness of examined composite floor systems. According to ISO/DIS 24322 (2023), the specimens were loaded at individual third point through a spreader beam using a 300-kN hydraulic jack and a 100-kN load cell. Two 50-mm diameter steel bars, loaded by a spreader beam, were placed on the position of the point loads to distribute load across the width of the specimen. Moreover, two LVDTs were used to measure the mid-span vertical deflections of floor specimen during the test. Experimental layout for four-point bending test was shown in Fig. 7. During each test, three initial load cycles of 1 kN were applied to the specimen to ensure the proper function of the instrumentation. After these cycles, the floor specimen was loaded until failure occurred in approximately 1 minute of loading for each test, referring to loading procedures in ISO/DIS 24322 (2023).

4.4 Creep test

The creep test was conducted on a composite floor specimen to investigate its behavior under long-term loading. The four-point bending scheme with a simply supported boundary condition was used on the test. Following the process, the magnitude of applied load was 25% of average maximum load obtained from bending test results. The load was idealized using a group of concrete blocks stacked on 10 wide flange spreader beams and centered relative to the behavior of the center of the gravity of the specimen. Each concrete block has been measured for its weight, to ensure that the total weight of the concrete blocks did not exceed 5% difference of the targetted load. Additionally, two 50-mm dial devices were placed at left and right sides of floor mid-span to measure vertical deflections during the examination. Referring to environmental requirements in ISO/DIS 24322 (2023), an air conditioner and humidifier were used to control room temperature and humidity at 25°C and 65%, respectively. The experimental layout for the creep test was shown in Fig. 8. Mid-span vertical deflections were measured for minimum of 90 days, according to ISO/DIS 24322 (2023).

Table 4 Recommended deflection measurement schedule (ISO/DIS 24322, 2023)

Event	Time of measurement (hr:min)
No load deformation immediately prior to loading	0:00
After loading is complete	0:01
	0:05
	0:10
	1:40
	8:20
One day after loading	24:00
Each day after loading, …	48:00, …

The measurement schedule referred to recommendations given in ISO/DIS 24322 (2023), as shown in Table 4. Creep factor obtained from the test was relative to the time of loading, and calculations were limited to 90-day. Therefore, logarithmic regression, by excluding the creep factor under 10 minutes of loading, was used to predict creep factor at a certain service life (ISO/DIS 24322, 2023).

5. Numerical model

Numerical models were applied to validate vibration and bending test results using ABAQUS software. The natural frequency, moment capacity, and flexural stiffness obtained from numerical analysis were compared to experimental results. Following the process, another objective of analysis aimed to investigate progressive flexural behavior of composite floor, which was difficult to observe in laboratory tests.

5.1 Material model and element type

The material model for CFS and plywood was idealized as an elasto-plastic material, without a damage criterion, based on bending test results that showed no damage or failure in either the CFS or plywood materials. On the other hand, this approach could also reduce the computational time of the model. The material model of CFS was idealized using the Ramberg-Osgood model developed by Gardner & Ashraf (2006) as elasto-plastic material, The constitutive equations of the Ramberg-Osgood model are given in Eqs. (1)-(2). Where E is the Young's modulus, $\sigma_{0.2}$ and $\sigma_{1.0}$ represented the 0.2% and 1% proof stress respectively, $E_{0.2}$ was the tangent modulus of stress-strain curve at $\sigma_{0.2}$, $\varepsilon_{0.2}$ and $\varepsilon_{1.0}$ represented the total strains corresponding to the 0.2% and 1.0% proof stress, while n as well as $n'_{0.2,1.0}$ are strain hardening exponents. The Young's modulus (E) and 0.2% proof stress ($\sigma_{0.2}$) were referred to as material properties of CFS in Table 1.

$$\varepsilon = \frac{\sigma}{E} + 0.002\left(\frac{\sigma}{\sigma_{0.2}}\right)^{n}; \text{ for } \sigma \le \sigma_{0.2} \quad (1)$$

$$\varepsilon = \frac{\sigma - \sigma_{0.2}}{E_{0.2}} + \left(\varepsilon_{1.0} - \varepsilon_{0.2} - \frac{\sigma_{1.0} - \sigma_{0.2}}{E_{0.2}}\right)\left(\frac{\sigma - \sigma_{0.2}}{\sigma_{1.0} - \sigma_{0.2}}\right)^{n'_{0.2,1.0}} + \varepsilon_{0.2}; \text{ for } \sigma_{0.2} < \sigma < \sigma_u \quad (2)$$

Plywood material was simplified as an isotropic instead of anisotropic material commonly used to model timber material. Elastic (modulus of elasticity) and plastic (compressive stregth for top plywood and tensile strength for bottom plywood) parameters were derived from the results of the plywood material tests in the laboratory, as shown in Table 2. Additionally, strengthened timber blocks and steel bars were modeled as elastic isotropic materials, with modulus elasticity and Poisson ratio of 12717.17 MPa and 0.33 for timber blocks (Dika Fajar *et al*. 2021, Tenar *et al*. 2017), and 200000 MPa and 0.3 for steel bars. Although CFS was commonly modeled as a shell element (Kyvelou *et al*. 2018), a three-dimensional solid element model was chosen in the analysis to model the interaction between CFS joists and plywood boards using epoxy-resin adhesives. All parts were assigned as 8-noded three-dimensional elements with reduced integration and hourglass control (C3D8R). Moreover, an appropriate mesh density should be chosen to capture accurate results and efficient computational time. Previous studies that conducted numerical analysis of CFS-timber board flooring systems under flexural loading have modeled CFS and timber board by using mesh density of 10 mm and 20 mm, respectively (Karki *et al*. 2021, Kyvelou *et al*. 2018). Considering the thickness of the CFS and plywood materials used in this study were smaller, the mesh density used is 5 mm and 10 mm, respectively. For the record, support and loading steel bars were not modeled in frequency analysis to avoid analyzing the natural frequency of those elements.

5.2 Contact modeling

At the position of support and loading points, strengthened timber blocks were tied to CFS joists, simulated self-drilling screw action in experimental specimens. The interactions between the support and loading points steel bars and the plywood boards were idealized as hard contact with a Coulomb friction coefficient set to 0.2, according to Kyvelou *et al*. (2018). Subsequently, the interaction between cold-formed steel joists, epoxy-resin adhesive, and plywood boards was modeled as a cohesive contact. In ABAQUS, there are two methods to modeling the behavior of the epoxy-resin adhesive, namely cohesive element and cohesive behavior. Both methods were based on traction-separation law to determine the bond-slip relationship, as shown in Eq. (3)

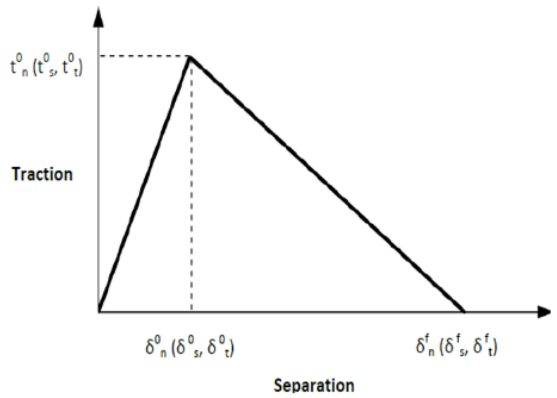

Fig. 9 Traction-separation law (ABAQUS 2018)

And Fig. 9. The difference between these two approaches is whether or not the adhesive layer is modeled. In the cohesive element approach, the adhesive layer was modeled so that failures due to adhesive separation could be observed. However, this approach requires a long computational time. Therefore, the cohesive behavior approach was used in this paper. Since this approach did not model the adhesive layer, the failures were observed through the traction value at the surfaces of two bonded elements.

$$\begin{Bmatrix} t_n \\ t_s \\ t_t \end{Bmatrix} = \begin{bmatrix} K_{nn} & 0 & 0 \\ 0 & K_{ss} & 0 \\ 0 & 0 & K_{tt} \end{bmatrix} \begin{Bmatrix} \delta_n \\ \delta_s \\ \delta_t \end{Bmatrix} \quad (3)$$

Where t_n, t_s, and t_t were tractions in normal and shear directions respectively, K_{nn} represented the normal cohesive stiffness, while K_{ss} and K_{tt} were the shear cohesive stiffness. The stiffness parameters were obtained using Eqs. (4)-(5), according to Ngudiyono *et al.* (2021). Where τ_{max} was the maximum shear stress and s_1 was the slip when the maximum shear stress occurred. Moreover, the tractions in normal and shear parameters were referred to as adhesive shear strength obtained from laboratory shear tests. The cohesive behavior key parameters used to model the interaction between CFS and plywood boards are presented in Table 5. Due to the lack of laboratory test data, the interaction between the plywood boards was also modeled as cohesive behavior with the parameters referring to 12-mm thick plywood-CFS interaction.

$$K_{ss} = K_{tt} = \frac{\tau_{max}}{\delta_1} \quad (4)$$

$$K_{nn} = 100 K_{ss} \quad (5)$$

5.3 Boundary conditions

In laboratory tests, the support steel bars were placed on steel beams; therefore, fixed boundary conditions were applied to the bottom surface of the modeled support steel bars. To capture floor behavior beyond ultimate load, the load was introduced by using controlled displacement boundary conditions applied at reference point created at the mid-span of the composite floor and constrained to loading point steel bars. Frequency linear pertubation and general static analysis were used to obtain frequencies and load-deflection curve of floor model. These two parameters were compared to the experimental results of the study.

Table 5 Cohesive behavior parameters

Parameters	12-mm thick plywood-CFS	18-mm thick plywood-CFS
K_{nn} (N/mm)	160.45	175.44
$K_{ss} = K_{tt}$ (N/mm)	1.60	1.75
$t_n = t_s = t_t$ (N/mm^2)	1.73	2.17

Table 6 First natural frequency comparison of experimental and numerical analysis results

Method	Natural frequency, f_1 (Hz)	Difference* (%)
Exp. Sampling 1	25.78	6.2
Exp. Sampling 2	25.68	6.6
Exp. Sampling 3	25.49	7.4
Numerical analysis	27.37	-

**Numerical analysis difference to each experimental result*

6. Results and discussion

6.1 Natural frequency

Time history functions obtained from three repetitions of vibration tests were transformed to the frequency domain using Fast Fourier Transform (FFT) method. From FFT, shown in Table 6 and Fig. 10(a), the first natural frequencies ($f_{1,exp}$) were obtained as the frequency at maximum acceleration amplitude. Moreover, the average first natural frequency of the examined CFS-plywood composite floor system was 25.65 Hz in flexural mode. The first mode of the vibration obtained from numerical analysis, characterized by flexural mode as shown in Fig. 10(b), was found to have a natural frequency ($f_{1,FE}$) of 27.37 Hz, which matched the results obtained from vibration tests. The difference in first frequency between experimental and numerical analysis results was probably caused by the fact that the real body was not unconstrained (the specimen was placed on the soft rubber pad on the support). However, the errors were in the acceptable range of 6.2–7.4%, which showed good agreement between experimental and numerical model.

6.2 Failure mechanism and load-deflection behavior

All three specimens experienced in-plane brittle failure, similar to the experimental results by Držečnik *et al.* (2022), who examined timber-glass composite beams using epoxy-resin adhesive. The failure occurred due to epoxy-resin adhesive separation at the interface between CFS and

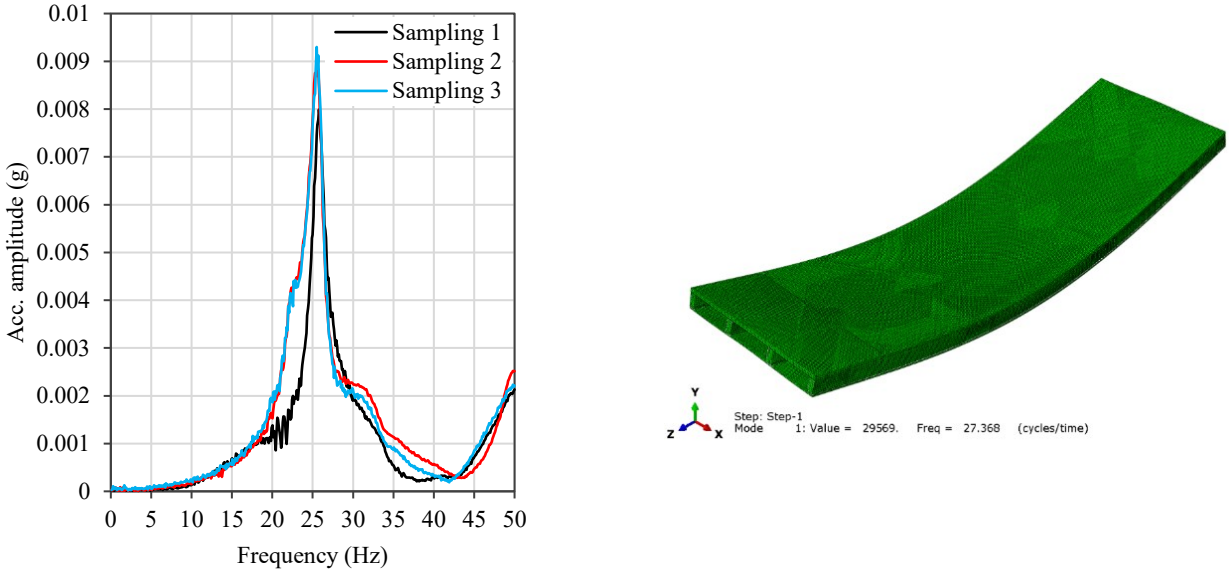

(a) Experimental results (b) Numerical analysis results

Fig. 10 First natural frequency of CFS-plywood composite floor system

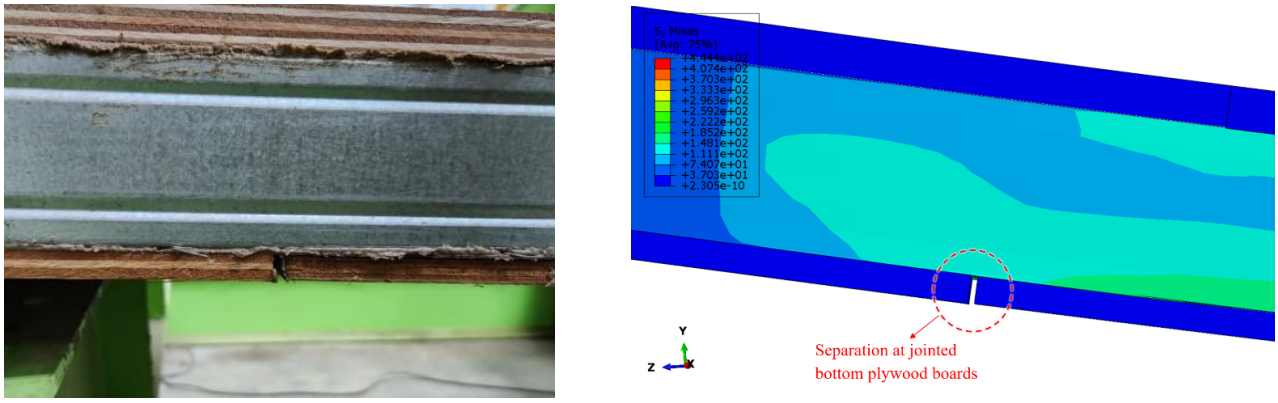

(a) Experimental results (b) Numerical analysis results

Fig. 11 Separation at jointed bottom plywood interfaces

bottom plywood at one of the shear spans as presented in Fig. 12(a). At the other shear span, separation occurred at the jointed bottom plywood interfaces, as shown in Fig. 11(a). The asymmetrical failure in both shear spans was probably caused by the uneven distribution of adhesive material on bonded surfaces.

Compared to numerical analysis results, the separation at the jointed bottom plywood interfaces occurred at 53% of maximum loading as shown in Fig. 11(b). Meanwhile, Fig. 12(b) showed the separation at the interface between CFS and bottom plywood occurred at 100% of maximum loading, indicated by the contact shear value that reached the adhesive shear strength of ≈1,73 MPa. These failure mechanisms indicate that the employed numerical analysis could capture the behavior of the examined composite floor system under flexural loading, even numerical analysis could provide more detail and progressive failure information.

Since strain gauges were not employed in laboratory bending tests, stress distribution at the CFS joists and plywood boards could not be observed. However, through visual observation, failures did not occur in these two parts. These observations were validated by the numerical analysis results shown in Figs. 13 and 14, where the stresses in the CFS, bottom plywood board, and top plywood board have not reached their yield, tensile, and compressive strength respectively.

The load-deflection data series obtained from bending tests were plotted to load-deflection curve, as demonstrated in Fig. 15. The deflection values plotted were obtained as average deflection of measurement of two LVDTs at left and right sides of each specimen. From load-deflection curves of all specimens, the slopes tended to be linear with a small degradation in stiffness, until reaching the maximum load followed by a sudden drop in load (brittle failure), sginifying that the specimens have failed. The maximum load of each specimen was taken to calculate the moment capacity (M_{exp}) of the CFS-plywood floor system, as presented in Table 7. Meanwhile, load-deflection data series up to the elastic limit, including 25% of the

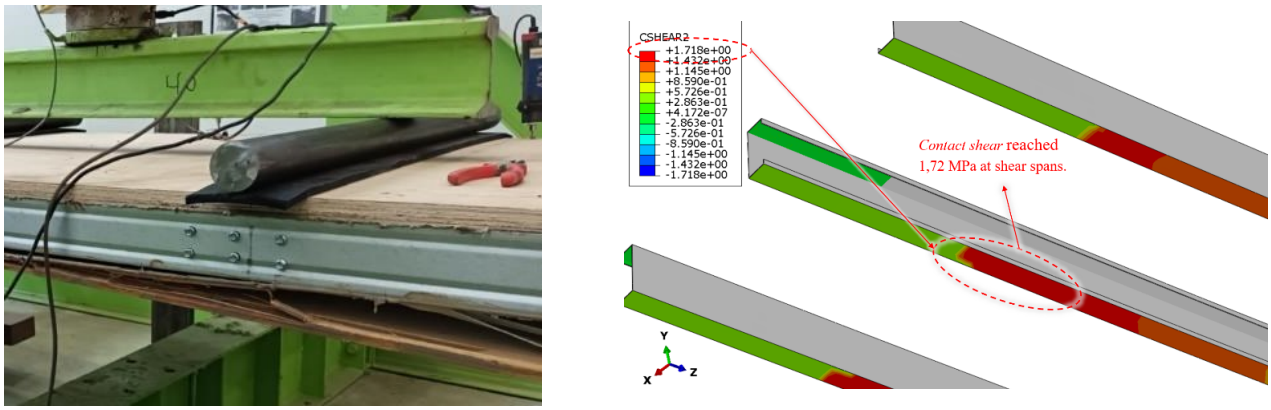

(a) Experimental results (b) Numerical analysis results

Fig. 12 Epoxy-resin adhesive shear failure at the cold-formed steel-bottom plywood interface

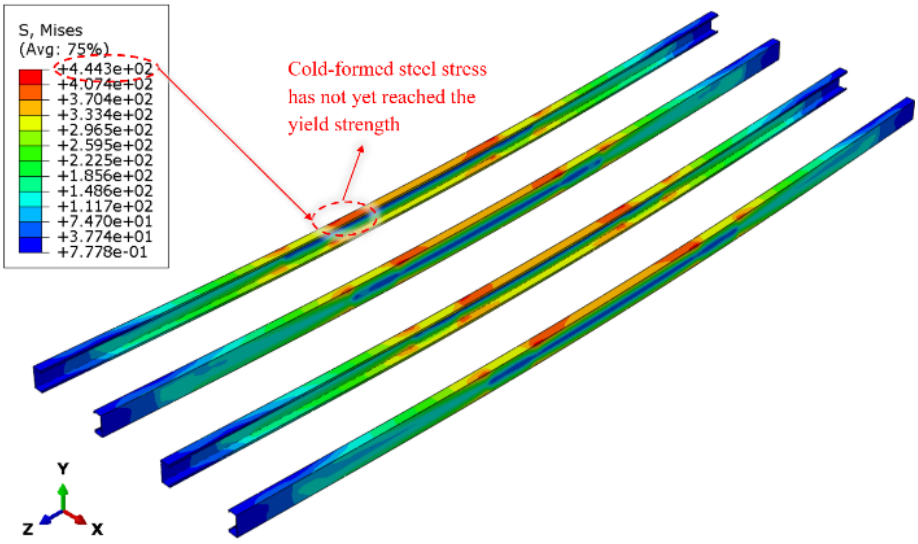

Fig. 13 Stress distribution of cold-formed steel joists at maximum loading

Table 7 Moment capacity and flexural stiffness of experimental and numerical analysis results

Method	Moment capacity, M		Flexural stiffness, EI	
	(kNm)	Difference* (%)	(kNm^2)	Difference* (%)
Exp. Specimen 1	18.76	0.4	369.16	4.7
Exp. Specimen 2	20.00	5.8	366.37	5.5
Exp. Specimen 3	17.03	10.6	374.35	3.3
Numerical analysis	18.84	-	386.64	-

**Numerical analysis difference to each experimental result*

maximum load (Kyvelou *et al*. 2015), was used to calculate the flexural stiffness ($(EI)_{exp}$). The flexural stiffness was later used to calculate deflection in serviceability limit state evaluation.

From bending tests, average moment capacity and flexural stiffness of the examined CFS-plywood composite floor system are 18.60 kNm and 369.96 kNm^2 respectively. Compared to experimental results, numerical model provided analysis results that simulated the ideal behavior of CFS-plywood composite floor system under flexural loading. Stiffness degradation due to micro-failures in the model was not visible in load-deflection curve. This result was due to the assumption of uniform bond of adhesive materials without any manufacturing defects, leading to a higher value of flexural stiffness ($(EI)_{FE}$) of 386.64 kNm^2 than the experimental with 4.7–5.5% differences. Concerning moment capacity, numerical analysis results (M_{FE}) of 18.84 kNm were close to experimental specimen 1 with a difference of 0.4%, while compared to specimen 2 and specimen 3, the numerical analysis results were still in the acceptable range of differences, i.e., 5.8% and 10.6% respectively.

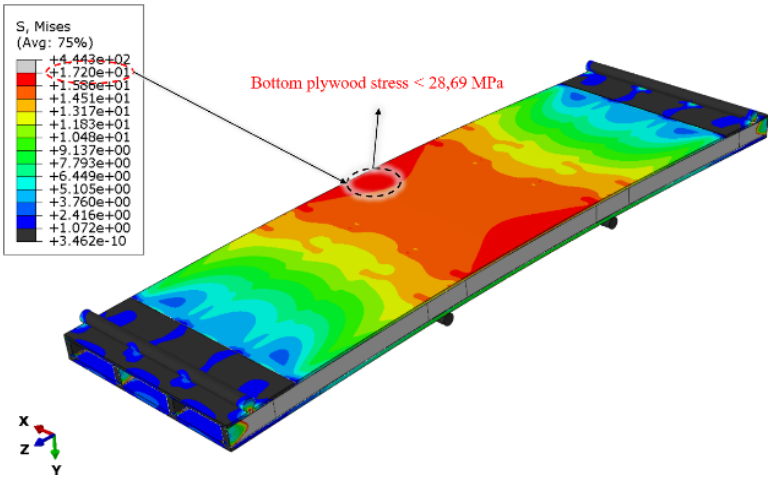

(a) Bottom Meranti plywood

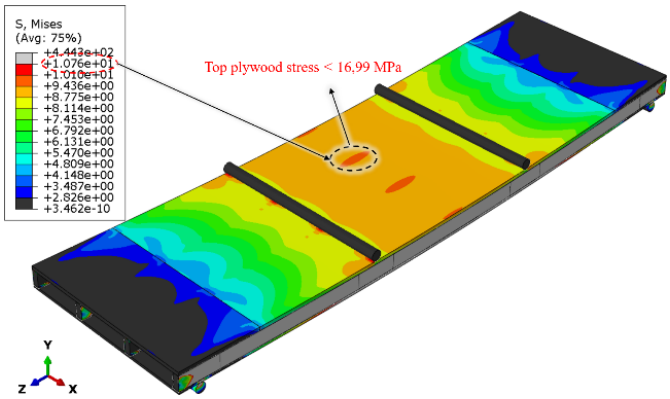

(b) Top Meranti-Sengon plywood

Fig. 14 Stress distribution of plywood boards at maximum loading

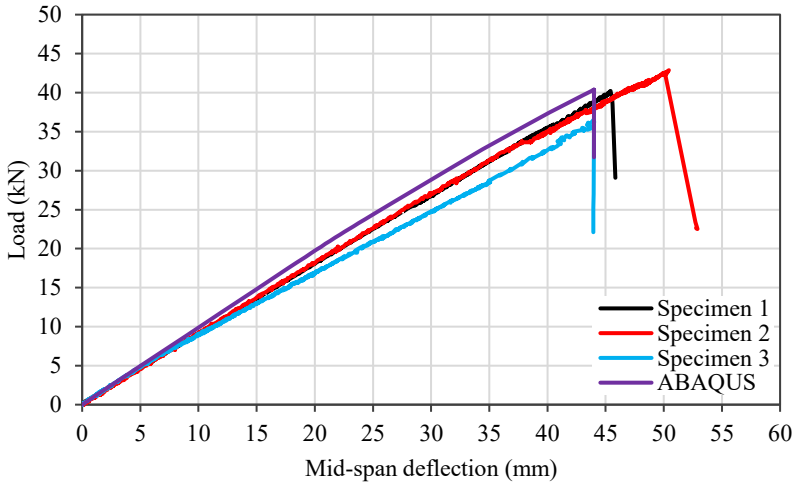

Fig. 15 Load-deflection curve of experimental and numerical analysis results

6.3 Long-term behavior and creep factor

A specimen of CFS-plywood composite floor system was used in the experimental creep test. The magnitude of the applied load was 25% of the average maximum load obtained from the bending test results. According to the average maximum load of 39.87 kN obtained from the bending test, 9.96 kN should applied in the creep test. Therefore, the total weight of wide flange spreader beams and stacked concrete blocks of 1019.7 kg (10 kN) was close to this requirement by only 0.3% difference. Measurement of deflection and calculation of the creep factor at each measurement time was carried out for 90 days. The average deflection was taken from two dial gauges, one each on the

Table 8 Design loads for CFS-plywood composite floor evaluation

Load type	Distributed load (kN/m)
Self-weight (DL)	
- Four cold-formed steel beams	0.047
- Meranti plywood	0.063
- Meranti-Sengon plywood	0.067
SPC-type floor covering (DL)	0.080
Live load for residential building (LL)	1.728

Table 9 Ultimate and serviceability limit state evaluation results

Parameters	Value and requirement	Check
Ultimate limit state		
- Moment capacity	18.60 kNm > 3.01 kNm	Passed
Serviceability limit state		
- Total deflection	4.88 mm < 11.67 mm	Passed
- Vibration	25.65 Hz > 8Hz; 9Hz	Passed

left and right sides of the specimen. The time-deflection relationship obtained from the creep test is presented in Fig. 16.

Deflection measurement showed that an instant deflection of 10.93 mm occurred after 1 minute of 10 kN loading was completed. Subsequently, the deflection increased rapidly until 9 hours after loading, reaching 11.82 mm, showing a slightly increasing trend until the 34th day after loading, where it increased from 11.82 mm to 12.51 mm. The increase in deflection was very small from 12.51 mm on day 34 to 12.57 mm on 90th day. When looking at the change in deflection from day 0 (instant bend) to 90, it only increased by 1.64 mm. These findings were consistent with the study conducted by Chiniforush *et al*. (2019), who investigated the behavior of a hot-rolled steel-CLT composite system under a constant load equivalent to 27% of the maximum bending load for 16 months. The results showed that the difference between the instant and final deflection at the 16th month was only 0.8 mm.

From the deflection measurement data, the creep factor at day 90 was 0.15, which was relatively small compared to the 2.0 creep factor for structural wood given in Indonesian National Standard 7973:2013 (SNI 7973 2013). This finding was probably due to the existence of CFS, which had a very low viscosity relative to plywood. During the study, creep factor found was similar to the test results by Chiniforush *et al*. (2021), where the creep factor of the hot-rolled steel-CLT composite system at the 22nd month of loading was 0.19.

Since creep factor value changed relative to time, the creep factor on the 90th day of loading could not be used as a design reference, considering that service life of buildings generally was 50 years. In ISO/DIS 24322 (2023), creep factor for specified service life could be estimated using logarithmic regression line, excluding the creep factor under 10 minutes of loading. According to regression equation in Fig. 17, the predicted creep factor for a 50-year service life was 0.24, greater than the creep factor of the 90th day of loading. The predicted creep factor was then used in calculation of total deflection to evaluate serviceability limit state of CFS-plywood composite floor system.

6.4 Composite floor system evaluation for residential buildings

In building design, especially for flooring systems, the design was not only limited to the strength of the floor system, but also its serviceability, including deflection and vibration. Through comprehensive experimental tests, moment capacity, total deflection, and vibration were obtained to be evaluated for residential building design loads. The applied loads in the examinations included self-weight of composite floor, additional dead load of floor covering, and live load for the residential building function. The self-weight of the composite floor consisted of four CFS beams, Meranti plywood, and Meranti-Sengon plywood, which were calculated based on the density and dimensions of each material. The additional dead load of floor covering from a 4 mm thick SPC was 9.11 kg/m^2. Meanwhile, live load for residential buildings refers to Indonesian National Standard (SNI 1727 2020), including 1.92 kN/m^2. All applied loads were then converted to distributed loads per meter, assuming floor width 900 mm as presented in Table 8.

For ultimate limit states evaluation, a load combination of 1.2DL + 1.6LL was used to compute factored moment. The result showed that factored moment of the CFS-plywood composite floor system for residential buildings is 3.01 kNm. According to average moment capacity system of 18.60 kNm, the CFS-plywood composite floor system had a safety factor of 6.2, greater than safety factor obtained in study by Wood (1960) of 1 to 4.

Deflection of simply supported CFS-plywood composite floor system was calculated using design loads, span length, and average flexural stiffness obtained from bending tests. Concerning the long-term behavior of plywood material,

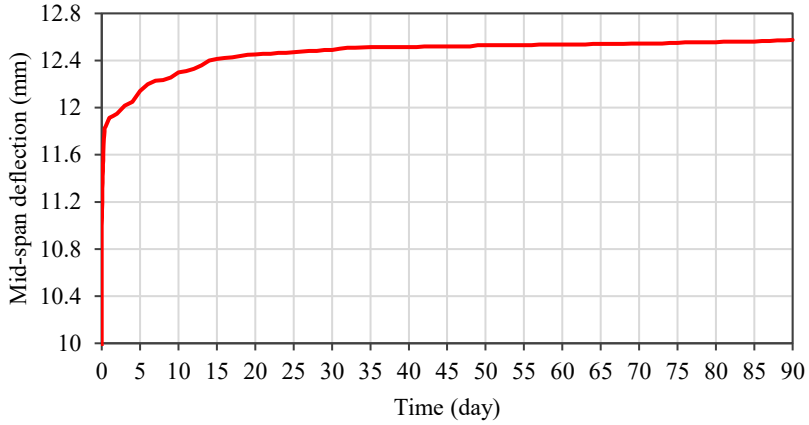

Fig. 16 Time-deflection curve of creep test results

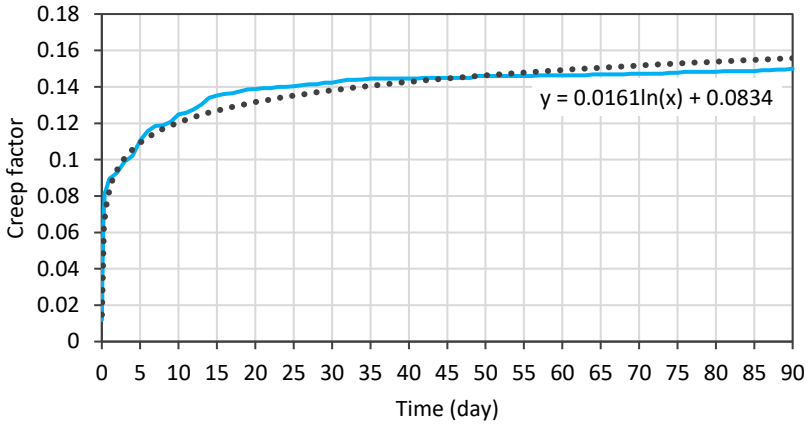

Fig. 17 Logarithmic regression line of time-creep factor curve

calculated deflection was captured as the sum of the deflection due to short-term and long-term load combinations (SNI 7973, 2013). Load combinations of 1.0DL + 1.0LL and 1.0DL + 0.5LL were used to calculate the short-term and long-term deflections respectively. During the study, 50-year service life creep factor of 0.24 was then used as a multiplying factor for long-term deflection. From the calculation, the total deflection of CFS-plywood composite floor system for residential buildings was 4.88 mm, less than maximum deflection limit of 11.67 mm (*l*/240).

Some human activities imparted dynamic forces to the floor system in the frequency range of 2 Hz to 6 Hz (Allen and Rainer 1976). When the natural frequency of a floor system was in this range and human activity on it was rhythmic, then resonance amplification might occur. Eurocode 5 (EN 1995-1-1 2004) and AISC design guide 11 (AISC 2016) limited minimum natural frequency of 8 Hz and 9 Hz, respectively, to prevent the resonance that could lead to user discomfort. According to vibration test results, average natural frequency of 25.65 Hz of CFS-plywood composite floor system has met minimum values of 8 Hz and 9 Hz. Based on the results of ultimate and serviceability limit state evaluations presented in Table 9, the examined CFS-plywood composite floor system was safe to use in residential buildings.

5. Conclusions

This study has comprehensively investigated the structural behavior of a cold-formed steel-plywood composite floor system using epoxy-resin adhesive connections. Through an extensive series of experimental tests, including vibration, bending, and creep evaluations, the floor system demonstrated excellent performance under both ultimate and serviceability limit states.

In terms of the ultimate limit state, the floor system demonstrated in-plane brittle failure modes. These were characterized by epoxy-resin adhesive separation at the interface between CFS and bottom plywood, as well as at the jointed plywood interfaces. Despite these localized failures, the system exhibited an average moment capacity of 18.60 kNm, significantly exceeding the factored design moment of 3.01 kNm. This result provided a safety factor of 6.2, demonstrating the structural robustness and reliability of the system under the applied loads typical of residential buildings. The excellent moment capacity performance highlights the suitability of the system for resisting ultimate loading conditions.

Concerning serviceability limit state, the floor system exhibited exceptional dynamic characteristics, with an average natural frequency of 25.65 Hz, substantially higher than the minimum comfort thresholds of 8 Hz and 9 Hz

specified in international standards. The flexural stiffness of 369.96 kNm² ensured that the total deflection, including the predicted creep factor of 0.24 over a 50-year service life, was 4.88 mm. This value was well below the allowable limit of 1/240 of floor span, reflecting the system's capacity to maintain serviceability and user comfort under both short- and long-term loading conditions.

Numerical analysis developed in this study not only successfully validated the experimental results but also provided deeper insights into the structural behavior of the composite floor system. The analysis demonstrated excellent agreement with experimental findings, showing differences of only 0.4%–10.6% for moment capacity, 3.3%–5.5% for flexural stiffness, and 6.2%–7.4% for natural frequency. This level of accuracy underscores the reliability of the numerical model in replicating real structural performance. The numerical simulations captured critical behaviors, including progressive failure mechanisms such as stress distribution and adhesive shear failure, which were challenging to observe in laboratory tests. Beyond validation, the numerical models offer significant potential for advanced parametric studies. They provide a platform for exploring a wide range of design variables, such as span lengths, cross-sectional dimensions, adhesive properties, and material configurations. These studies can help optimize the floor system's performance, adapt it to various structural requirements, and explore its application in more demanding scenarios.

In conclusion, the innovative CFS-plywood composite floor system developed in this research offers a lightweight, structurally robust, and sustainable solution for residential building applications. Its compliance with both ultimate and serviceability criteria highlight its potential for practical implementation in modern construction. Future work could also explore broader applications in multi-story buildings or more demanding structural designs to further expand its versatility and impact.

Acknowledgments

The authors would like to thank Jarwanto Nugroho, Sukino, Haryanta, and Eko Suroyo for their support and work in the laboratory.

References

ABAQUS (2018), *Analysis User's Guide Volume V: Element*.

Sheta, A.M., Ma, X., Zhuge, Y., ElGawady, M.A., Mills, J.E. and Abd-Elaal, E.S. (2023), "Shear behaviour of thin-walled composite cold-formed steel/PE-ECC beams", *Steel Compos. Struct. Int. J.*, **46**(1), 75-92.

AISC. (2016), *Steel Design Guide Vibrations of Steel-Framed Structural Systems Due to Human Activity Second Edition*.

Akbar, M.K., Awaludin, A. and Triwiyono, A. (2024), "Studi eksperimental dan analisis empirik performa sambungan sistem lantai komposit cold formed steel-plywood", *Proceeding Civil Engineering Research Forum*, 205–217.

Al Hunaity, S., Far, H. and Saleh, A. (2022), "Vibration behaviour of cold formed steel and farticleboard composite flooring systems", *Steel Compos.Struct. Int. J.*, **43**, 403-417. https://doi.org/10.12989/scs.2022.43.3.403.

Allen, D.E. and Rainer, J.H. (1976), „Vibration criteria for long-span floors", *Can. J. Civil Eng.*, **3**, 165-173. https://api.semanticscholar.org/CorpusID:111246291.

Altmann, R.E., Atadero, R. and Valdes -Vasquez, R. (2022), "CO2eq comparison between a light gauge steel framing structure and a CMU structure for single-family residential projects in Costa Rica", *EPiC Ser. Built Environ.*, **3**, 740–748.

American Institute of Steel Construction. (2011), *AISC Steel Construction Manual*.

Australian Standards. (1993), *AS 3623: Domestic Metal Framing*.

Awaludin, A., Adiyuano, Y. and Mursyid, F.A. (2020), "RISBARI: An alternative house model for the 2018 Lombok earthquake affected people", *IOP Conf. Ser. Mater. Sci. Eng.*, **849**(1). https://doi.org/10.1088/1757-899X/849/1/012069.

Chiniforush, A.A., Valipour, H.R., Bradford, M.A. and Akbar Nezhad, A. (2021), "Experimental and theoretical investigation of long-term performance of steel-timber composite beams", *Eng. Struct.*, **249**, 113314. https://doi.org/10.1016/j.engstruct.2021.113314.

Chiniforush, A.A., Valipour, H.R., Bradford, M.A. and Akbarnezhad, A. (2019), "Long-term behaviour of steel-timber composite (STC) shear connections", *Eng. Struct.*, **196**, 109356. https://doi.org/10.1016/j.engstruct.2019.109356.

Karki, D., Far, H. and Al-hunity, S (2022), "Determination of slip modulus of cold-formed steel composite members sheathed with plywood structural panels", *Steel Compos. Struct. Int. J.*, **43**(4), 511-522.

Fajar, R.D., Sutandar, E. and Supriyadi, A. (2021), "Identifikasi Kuat Acuan Jenis Kayu yang Diperdagangkan berdasarkan SNI 7973: 2013", *JeLAST: Jurnal Teknik Kelautan, PWK, Sipil, dan Tambang*, **8**(1). https://doi.org/10.26418/jelast.v8i1.44610.

Držečnik, M., Štrukelj, A. and Premrov, M. (2022), "Influence of the bonding boundary conditions of timber-glass I-Beams on load-bearing capacity and stiffness", *Appl. Sci.*, **12**(4), 1770. https://doi.org/10.3390/app12041770.

EN 789 (2004), *Timber structures - Test Methods - Determination of Mechanical Properties of Wood Based Panels*.

EN 1995-1-1 (2004), *EUROPEAN STANDARD Eurocode 5: Design of Timber Structures - Part 1-1: General - Common Rules and Rules for Buildings*.

Far, H. (2020), "Flexural behavior of cold-formed steel-timber composite flooring systems", *J. Struct. Eng.*, **146**(5). https://doi.org/10.1061/(asce)st.1943-541x.0002600.

Gardner, L. and Ashraf, M. (2006), "Structural design for non-linear metallic materials", *Eng. Struct.*, **28**(6), 926-934. https://doi.org/10.1016/j.engstruct.2005.11.001.

Hassanieh, A., Valipour, H.R., Bradford, M.A. and Sandhaas, C. (2017), "Modelling of steel-timber composite connections: Validation of finite element model and parametric study", *Eng. Struct.*, **138**, 35-49. https://doi.org/10.1016/j.engstruct.2017.02.016.

ISO/DIS 2432. (2023), *Timber structures - Method of Test for Evaluation of Long-Term Performance - Part 1: Wood-Based Products in Bending*.

Johnston, R.P.D., McGrath, T., Nanukuttan, S., Lim, J.B.P., Soutsos, M., Chiang, M.C., Masood, R. and Rahman, M.A. (2018), "Sustainability of cold-formed steel portal frames in developing countries in the context of life cycle assessment and life cycle costs", *Struct.*, **13**, 79-87. https://doi.org/10.1016/j.istruc.2017.11.003.

Karki, D., Al-Hunaity, S., Far, H. and Saleh, A. (2022), "Composite connections between CFS beams and plywood panels for flooring systems: Testing and analysis", *Struct.*, **40**, 771-785. https://doi.org/10.1016/j.istruc.2022.04.064.

Karki, D., Far, H. and Saleh, A. (2021), "Numerical studies into factors affecting structural behaviour of composite cold-formed

steel and timber flooring systems", *J. Build. Eng.*, **44**. https://doi.org/10.1016/j.jobe.2021.102692.

Kullit, R.A. (2013), "*PERILAKU CREEP BALOK LAMINATED VEENER LUMBER KAYU SENGON (Paraserianthes falcataria) DENGAN TUMPUAN KANTILEVER*", Doctoral Dissertation, Universitas Gadjah Mada.

Kyvelou, P., Gardner, L. and Nethercot, D.A. (2015), "Composite action between cold-formed steel beams and wood-based floorboards", *Int. J. Struct. Stab. Dyn.*, **15**(8), 1540029. https://doi.org/10.1142/S0219455415400295.

Kyvelou, P., Gardner, L. and Nethercot, D.A. (2018), "Finite element modelling of composite cold-formed steel flooring systems", *Eng. Struct.*, **158**, 28-42. https://doi.org/10.1016/j.engstruct.2017.12.024.

Kyvelou, P., Reynolds, T.P.S., Beckett, C.T.S. and Huang, Y. (2021), "Experimental investigation on composite panels of cold-formed steel and timber", *Eng. Struct.*, **247**, 113186. https://doi.org/10.1016/j.engstruct.2021.113186.

Lai, B.L., Li, Y.R., Jin, L. and Fan, S.G. (2024), "Experimental study on the compressive behavior of UHPC filled stainless steel tubes subjected to monotonic and cyclic loading", *Construct. Build. Mater.*, **449**, 138301. https://doi.org/10.1016/j.conbuildmat.2024.138301.

Lai, B.L., Zheng, X.F., Fan, S.G. and Chang, Z.Q. (2024), "Behavior and design of concrete filled stainless steel tubular columns under concentric and eccentric compressive loading", *J. Constr. Steel Res.*, **213**, 108319. https://doi.org/10.1016/j.jcsr.2023.108319.

Making, M.Y.M., Awaludin, A. and Supriyadi, B. (2021), "The effects on screw fasteners spacing on flexural behavior and strength capacity of cold-formed steel built-up box sections", *MEDIA KOMUNIKASI TEKNIK SIPIL*, **26**(2), 163-173. https://doi.org/10.14710/mkts.v26i2.31503.

Meyer, C. (2013), *The Greening of the Concrete Industry*.

Nashirudin, M., Basuki, A. and Supriyadi, A. (2016), "PERILAKU RANGKAK PADA BALOK LAMINATED VENEER LUMBER (LVL) KAYU SENGON", *Matriks Teknik Sipil*, **4**(1). https://doi.org/10.20961/mateksi.v4i1.37105.

Ngudiyono, N., Hariyadi, H. and Ningsih, Y.P. (2021), "SIMULASI NUMERIK KUAT LEKAT TULANGAN BAJA DAN BETON DENGAN PROGRAM ABAQUS STUDENT EDITION (SE)", *FROPIL (Forum Profesional Teknik Sipil)*, **9**(1), 10-17. https://doi.org/10.33019/fropil.v9i1.2287.

Suhendro, B., Awaludin, A. and Triwiyono, A. (2020), "Creep shear deformation of glued-laminated bamboo", *Int. J. GEOMATE*, **19**(73), 185-192. https://doi.org/10.21660/2020.73.42823.

Shamayleh, O. and Far, H. (2022), "Investigation on structural behaviour of composite cold-formed steel and reinforced concrete flooring systems", *Steel Compos. Struct. International J.*, **45**(6), 895-905. http://hdl.handle.net/10453/164590.

Pratiwi, N. and Tjondro, J.A. (2018), "Study on strength and stiffness of meranti wood truss with plywood gusset plate connection and lag screw fastener", *J. Civ. Eng. Forum*, **4**(1), 51. https://doi.org/10.22146/jcef.30230.

Raffoul, S., Heywood, M., Moutaftsis, D. and Rowell, M. (2019), "Experimental investigation of cold-formed steel-timber board composite floor systems", *Int. J. Struct. Constr. Eng.*, **13**(9), 509-514.

Różyło, P. (2023), "Failure analysis of beam composite elements subjected to three-point bending using advanced numerical damage models", *acta mechanica et automatica*, **17**(1), 133-144. https://doi.org/10.2478/ama-2023-0015.

SNI 1727 (2020), *Beban desain minimum dan kriteria terkait untuk bangunan gedung dan struktur lain*, Badan Standardisasi Nasional.

SNI 7973 (2013), *Spesifikasi desain untuk konstruksi kayu*, Badan Standardisasi Nasional.

Szewczak, I., Rzeszut, K., Rozylo, P. and Samborski, S. (2020), "Laboratory and numerical analysis of steel cold-formed sigma beams retrofitted by bonded CFRP tapes", *Mater.*, **13**(19), 4339. https://doi.org/10.3390/ma13194339.

Tenar, F.K., Mulyatno, I.P. and Budiarto, U. (2017), "Analisa Kekuatan Sambungan Konstruksi Lambung Pada Kapal Kayu 100 Gt Di Daerah Batang Dengan Menggunakan Metode Elemen Hingga", *Jurnal Teknik Perkapalan*, **5**(4), 641. http://ejournal3.undip.ac.id/index.php/naval.

Valsa Ipe, T., Sharada Bai, H., Manjula Vani, K. And Zafar Iqbal, M.M. (2013), "Flexural behavior of cold-formed steel concrete composite beams", *Steel Compos. Struct.*, **14**(2), 105-120. https://doi.org/10.12989/scs.2013.14.2.105.

Wood, L.W. (1960), "Factor of safety in design of timber structures", *Transact. American Soc. Civ. Eng.*, **125**(1), 1033-1045. https://doi.org/10.1061/TACEAT.0007921.

Wusqo, U., Awaludin, A., Setiawan, A.F. and Irawati, I.S. (2019), "Study of laminated veneer lumber (LVL) sengon to concrete joint using two-dimensional numerical simulation", *J. Civ. Eng. Forum*, **5**(3), 275. https://doi.org/10.22146/jcef.47694.

CC